

Judit Bartholy*, Rita Pongrácz, Ildikó Pieczka, Karolina Szabóné André
Dept. of Meteorology, Eötvös Loránd University, Budapest, Hungary

1. INTRODUCTION

In the framework of the Med-CORDEX international initiative (Ruti et al., 2016) of the CORDEX (Coordinated Regional Climate Downscaling Experiment) program within the WCRP (World Climate Research Program), our research group is contributing with RegCM4.3 experiments at 50 km horizontal resolution using the mosaic-type subgridding option in order to take into account subgrid processes. For this purpose, we used ERA-Interim data (1981-2010) and HadGEM2 global model outputs (1951-2005, 2006-2100) as initial and lateral boundary conditions (ICBC) for the entire MED-44 CORDEX area (Fig. 1) covering the extended Mediterranean region of Europe (30°-50°N, 10°W-45°E).

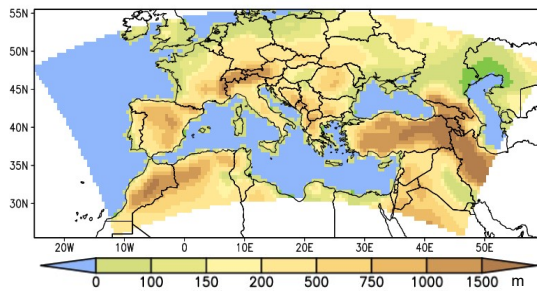


Fig. 1: The topography of the MedCORDEX integration domain for the RegCM4.3 simulation at 50 km horizontal resolution.

On the basis of 50 km RegCM runs we aim to provide detailed regional scale climate projection results for the Carpathian Region and its vicinity. For this purpose, further downscaling is necessary using 10 km as horizontal resolution for a smaller domain covering Central Europe with special focus on the Carpathian Region. These experiments will be the basis of the Hungarian national climate and adaptation strategies for detailed regional scale analysis and specific impact studies. The domain of our earlier fine resolution RegCM experiments (Bartholy et al., 2009; Pongrácz et al., 2010; Torma et al., 2011) has been substantially extended from 12000 gridcells to about 25000 gridcells, moreover, in the previous study we used RegCM3 model version, and emission scenarios (Nakicenovic and Swart, 2000) instead of the new Representative Concentration Pathways (RCP) scenarios (van Vuuren et al., 2011).

The model validation results are discussed in

Bartholy et al. (2015) and Pieczka et al. (2016) using two different ICBCs, (i) from datasets of ERA-Interim reanalysis, and (ii) from simulation outputs of HadGEM2 global climate model (GCM). After completing the historical experiments, future scenarios for the 21st century are run taking into account two very different scenarios (RCP4.5 and RCP8.5), which are based on the radiative forcing change by 2100 (van Vuuren et al., 2011). The projected temperature and precipitation changes on annual and seasonal scales are presented and compared in Pongrácz et al. (2016). This paper focuses on the projection results of extreme climatic conditions related to temperature and precipitation for the following 10 subregions (Fig. 2) defined within the MED-44 CORDEX integration domain: Iberian Peninsula (IP), Appennin Peninsula (AP), Balkan Region (BR), Asia Minor (AM), East European Plain (EEP), Middle European Plain (MEP), Carpathian Basin (CB), Carpathian Mountains (CM), Alps (A), Western Europe (WE).

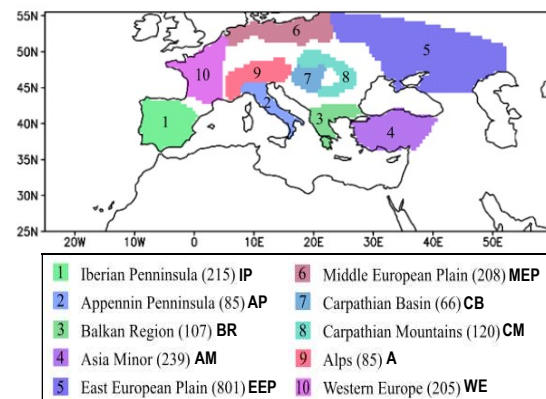


Fig. 2: Subregions within the integration domain defined for regional scale analysis for the 50-km model runs. The numbers appearing in parentheses after the name of the subregion indicate the total number of gridcells within the subregion.

2. REGIONAL CLIMATE MODEL REGCM

Regional climate model RegCM originally stems from the National Center for Atmospheric Research/ Pennsylvania State University (NCAR/PSU) Mesoscale Model version MM4 (Dickinson et al., 1989; Giorgi, 1989). It is a 3-dimensional, limited-area, hydrostatic, compressible, sigma-p vertical coordinate model

* Corresponding author address: Judit Bartholy, Dept. of Meteorology, Eötvös Loránd University, Pázmány st. 1/a. Budapest, H-1117; Hungary; e-mail: bartholy@caesar.elte.hu

maintained at ICTP (International Centre for Theoretical Physics), Trieste. It was originally developed by Giorgi et al. (1993a, 1993b) and later modified and improved by Giorgi and Mearns (1999) and Pal et al. (2000). Description of model equations and possible parameterizations available in the latest version can be found in Elguindi et al. (2011) in detail. In our simulations we used the model settings agreed as default within the Med-CORDEX project (Somot et al., 2012) at 50 km horizontal resolution, with the modification of activating the subgrid Biosphere-Atmosphere Transfer Scheme (BATS). Therefore, the land surface processes are modelled by BATS version 1e (Dickinson et al., 1993) with the treatment for subgrid variability of topography, and land cover is determined using a mosaic-type approach (Giorgi et al., 2003). Each grid cell is divided into 25 subgrid cells. As a result, in our simulation the size of the land surface grid cell is $10 \text{ km} \times 10 \text{ km}$ horizontally. The affect of the selection of the cumulus parametrization is discussed in Pieczka et al. (2016).

3. PROJECTION RESULTS

After completing the validation analysis (Bartholy et al., 2015; Pieczka et al., 2016) of the two different historical experiments using ERA-Interim reanalysis data and HadGEM2 GCM outputs as ICBC, the GCM simulation driven experiment continued with two different scenario conditions starting from 2006 throughout the entire 21st century. In order to analyze the simulation results, the projected temperature and precipitation changes are presented on annual and seasonal scales in Pongracz et al. (2016) and compared for the RCP4.5 and RCP8.5 scenarios.

In this paper the projected annual and seasonal mean changes of extremes climatic conditions related to temperature (in subsection 3.1) and precipitation (in subsection 3.2) are presented. The reference period is defined as the last two decades of the 20th century (1981-2000) in the whole study.

3.1 Temperature-related extremes

First, the estimated changes of cold conditions are analyzed. Fig. 3 shows the projected changes of the annual mean number of frost days (FD) when the daily minimum temperature is less than $0 \text{ }^\circ\text{C}$ ($T_{\min} < 0 \text{ }^\circ\text{C}$). The yellow and red colors of the maps indicate the future decrease of FD, which is a clear consequence of global and regional warming. The larger increase of radiative forcing (i.e., RCP8.5 assumes larger radiative forcing than RCP4.5) is projected to result in larger warming, and thus, a larger decrease of cold conditions. According to the climate model simulations, the European regional warming slows down in the second part of the 21st century in the case of RCP4.5 (e.g., Pongracz et al., 2016), which consequently results in very small differences between the projected decreases of FD in 2061-2080 and 2081-2099. Since RCP8.5 does not assume such change neither in the radiative forcing,

nor in the warming, the decrease of FD is projected to continue throughout the whole 21st century. Furthermore, the estimated mean decrease of FD is generally larger over the land than over the sea.

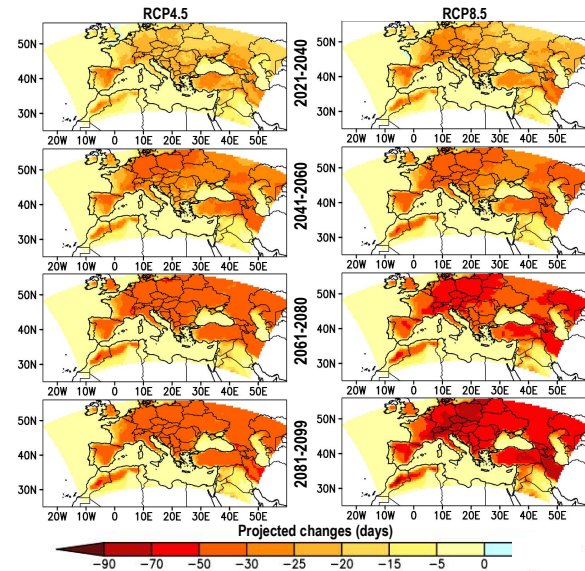


Fig. 3: Projected mean changes in the annual mean number of **frost days** (FD, $T_{\min} < 0 \text{ }^\circ\text{C}$) using the RCP4.5 (left panel) and RCP8.5 (right panel) scenarios. Reference period: 1981-2000.

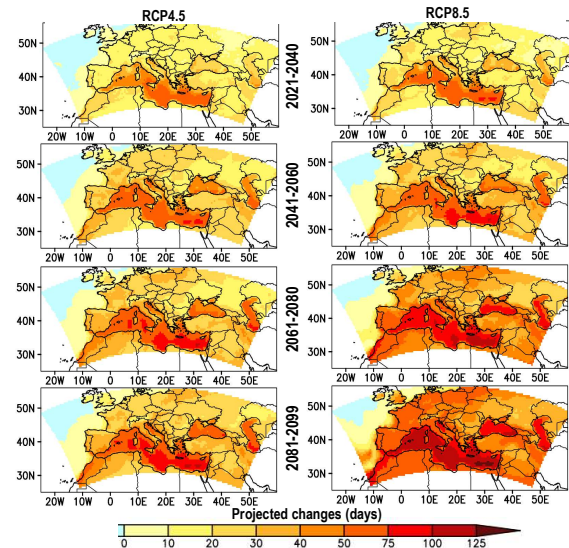


Fig. 4: Projected mean changes in the annual mean number of **summer days** (SU, $T_{\max} > 25 \text{ }^\circ\text{C}$) using the RCP4.5 (left panel) and RCP8.5 (right panel) scenarios. Reference period: 1981-2000.

Global and regional warming, i.e., the shift of temperature towards warmer conditions evidently results in higher occurrences of warm and hot conditions. Here, Fig. 4 shows the projected changes of the annual mean

number of summer days (SU) when the daily maximum temperature exceeds 25 °C ($T_{\max} > 25$ °C). Similarly to the projections in the case of FD, larger increase of radiative forcing and thus, larger global warming result in a larger change (here, increase) of warm conditions. Therefore, in the case of RCP8.5 a much larger increase of SU is projected by the end of the 21st century than in the case of RCP4.5. Note that the estimated increase of SU is substantially larger over the Mediterranean, the Black and the Caspian sea than over the continent. (The projected changes over the Atlantic are very small, which are similar to the changes of FD shown in Fig. 3.)

3.2 Precipitation-related extremes

The projected changes of precipitation-related extremes are certainly less straightforward from global and regional warming than the projected changes of temperature related extremes. Similarly to the temperature, two extreme indices (one negative, i.e., indicating the lack of precipitation, and one positive, i.e., indicating excessive precipitation) are selected in this paper. Because of the substantial differences in seasonal precipitation changes (Pongracz et al., 2016), the precipitation-related extreme indices are analyzed on a seasonal scale instead of the annual scale of temperature-related analysis. Warmer than usual climatic conditions together with the lack of precipitation may result in severe agricultural consequences in certain regions, and even economic losses (which can be prevented with appropriate adaptation).

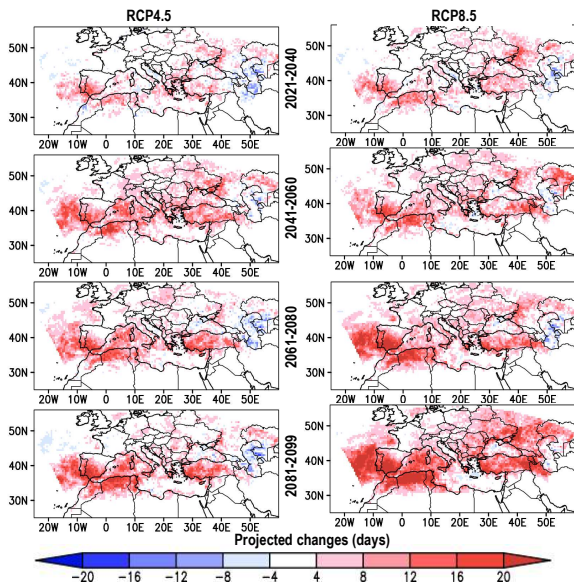


Fig. 5: The projected mean changes of **consecutive dry days** (CDD) in **summer** using the RCP4.5 (left panel) and RCP8.5 (right panel) scenarios. Reference period: 1981-2000.

Fig. 5 shows the projected mean changes of consecutive dry days in summer in the four periods of the 21st century. Unlike in the case of temperature-related indices, the differences between the two scenarios are much less. The overall drying affects the southern regions the most.

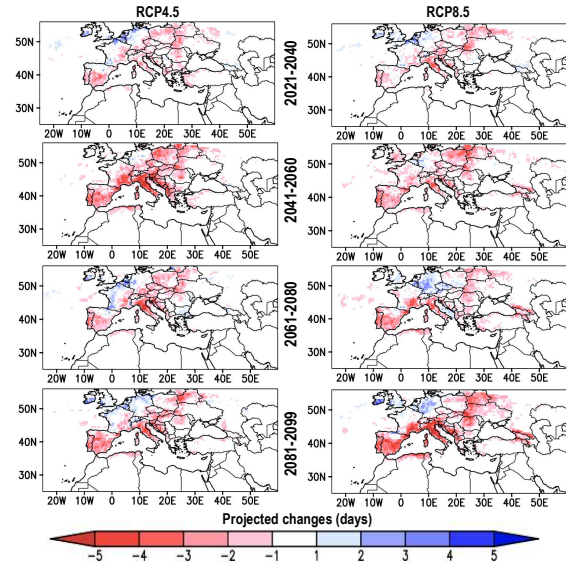


Fig. 6: The projected mean changes of **heavy precipitation days** (RR10) exceeding 10 mm/day in **summer** using the RCP4.5 (left panel) and RCP8.5 (right panel) scenarios. Reference period: 1981-2000.

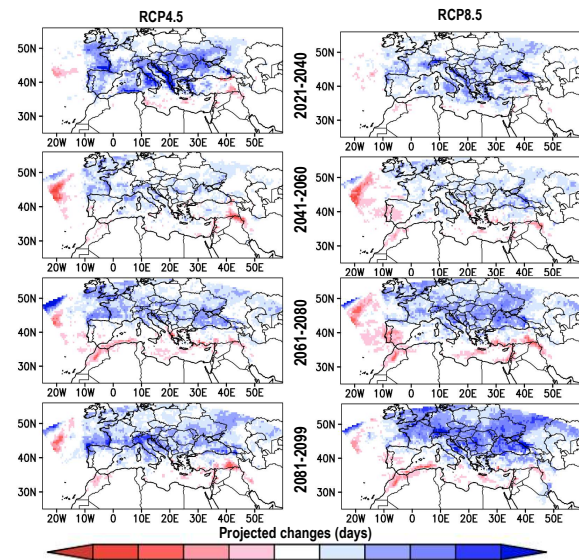


Fig. 7: The projected mean changes of **heavy precipitation days** (RR10) exceeding 10 mm/day in **winter** using the RCP4.5 (left panel) and RCP8.5 (right panel) scenarios. Reference period: 1981-2000.

Figs. 6 and 7 show the projected mean changes of heavy precipitation days (when the daily precipitation exceeds 10 mm, RR10) in summer and winter, respectively. Because of the asymmetric distribution of daily precipitation and the overall midlatitudinal climatic conditions in the area, this event is not too frequent, the estimated average changes range generally between -5 days/season and +5 days/season (much less than the changes of CDD). The maps indicate that most of the changes will occur over the continental area both in summer and winter, however, the projected changes are generally opposite in the two seasons; a decrease of RR10 is estimated in summer (except in the northwestern continental part of the domain), and an increase of RR10 is estimated in winter (except in the southwestern continental part of the domain).

For detailed regional scale analysis Box-Whisker diagrams are used to illustrate the distribution of the seasonal mean values of climatic indices in four different 20-year-long time slices for the future (i.e., 2021-2040, 2041-2060, 2061-2080, and 2081-2099), and thus compared to the reference period of 1981-2000. The diagrams indicate the whole range of the interannual variability (whiskers), and the simulated values around the mean represented by the upper and the lower quartiles (thicker boxes).

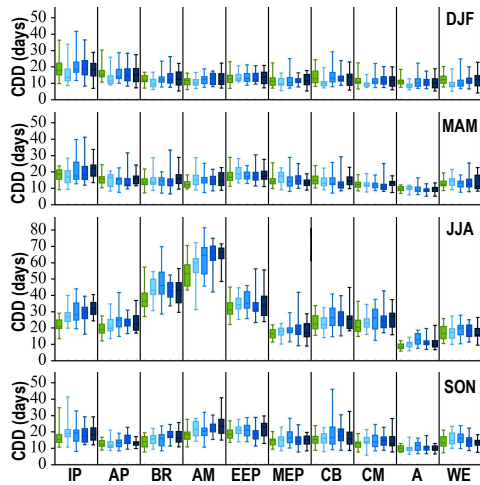


Fig. 8: The Box-Whisker diagrams of spatial average CDD values in the 10 subregions of the MED-44 CORDEX domain calculated from the **RCP4.5** scenario experiments. The presented time slices (indicated from green to dark blue) are 1981-2000, 2021-2040, 2041-2060, 2061-2080, 2081-2099. The diagrams indicate the whole range of interannual variability (thinner lines), and the simulated values around the mean represented by the upper and lower quartiles (thicker boxes).

Figs. 8 and 9 compare the seasonal simulated CDD values averaged over the 10 subregions throughout the 21st century for RCP4.5 and RCP8.5, respectively.

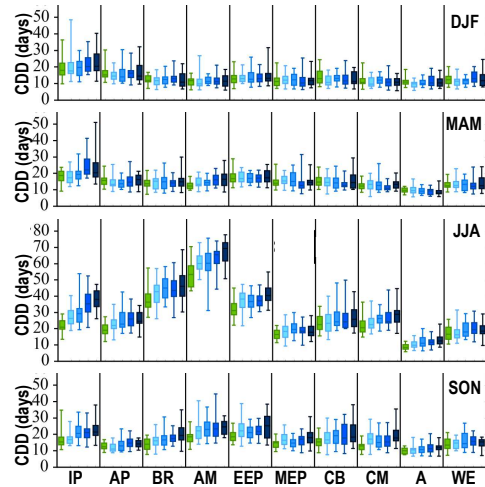


Fig. 9: The Box-Whisker diagrams of spatial average CDD values in the 10 subregions of the MED-44 CORDEX domain calculated from the **RCP8.5** scenario experiments. The presented time slices (indicated from green to dark blue) are 1981-2000, 2021-2040, 2041-2060, 2061-2080, 2081-2099. The diagrams indicate the whole range of interannual variability (thinner lines), and the simulated values around the mean represented by the upper and lower quartiles (thicker boxes).

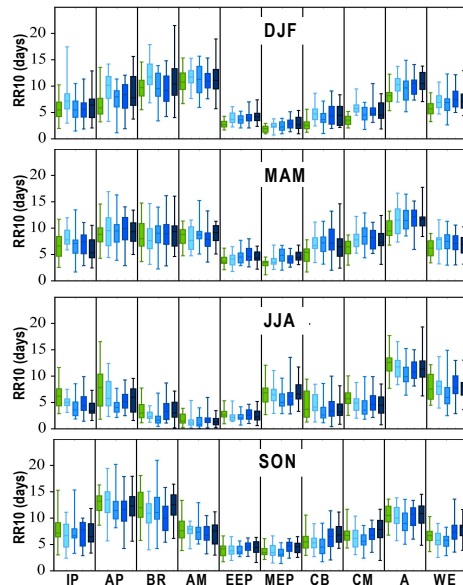


Fig. 10: The Box-Whisker diagrams of spatial average RR10 values in the 10 subregions of the MED-44 CORDEX domain calculated from the **RCP4.5** scenario experiments. The presented time slices (indicated from green to dark blue) are 1981-2000, 2021-2040, 2041-2060, 2061-2080, 2081-2099. The diagrams indicate the whole range of interannual variability (thinner lines), and the simulated values around the mean represented by the upper and lower quartiles (thicker boxes).

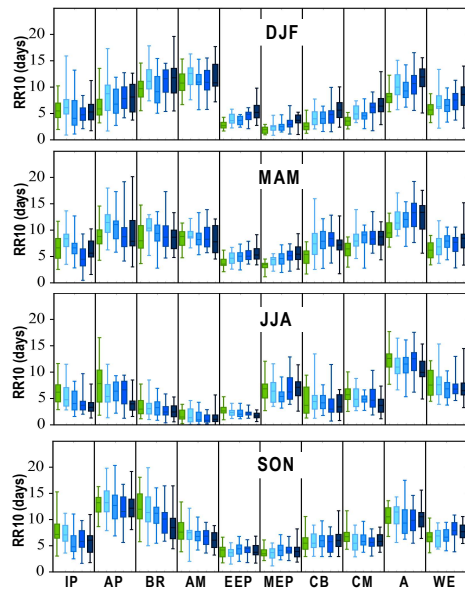


Fig. 11: The Box-Whisker diagrams of spatial average RR10 values in the 10 subregions of the MED-44 CORDEX domain calculated from the RCP8.5 scenario experiments. The presented time slices (indicated from green to dark blue) are 1981-2000, 2021-2040, 2041-2060, 2061-2080, 2081-2099. The diagrams indicate the whole range of interannual variability (thinner lines), and the simulated values around the mean represented by the upper and lower quartiles (thicker boxes).

Figs. 10 and 11 compare the seasonal simulated RR10 values averaged over the 10 subregions throughout the 21st century for RCP4.5 and RCP8.5, respectively.

Acknowledgements. Research leading to this paper has been supported by the following sources: the AGRÁRKLIAM2 project (VKSZ_12-1-2013-0034), the AgroMo project (GINOP-2.3.2-15-2016-0002), the Hungarian Scientific Research Fund under grants K109109 and K-120605, and the EEA Grant HU04 Adaptation to Climate Change Programme (EEA-C13-10).

REFERENCES

- Bartholy, J., Pongrácz, R., Torma, Cs., Pieczka, I., Hunyady, A., 2009: Regional climate model experiments for the Carpathian basin. In: *Proceedings, 89th AMS Annual Meeting*. Phoenix, AZ. Paper 13A.03, 5p. Available online at <http://ams.confex.com/ams/pdfpapers/147084.pdf>
- Bartholy, J., Pongrácz, R., Pieczka, I., Kelemen, F.D., Kís, A., André, K., 2015: Regional climate model experiment using RegCM subgridding options in the framework of Med-CORDEX. In: *Proceedings, 95th AMS Annual Meeting*. Phoenix, AZ. Paper 591, 6p. Available online at <https://ams.confex.com/ams/95Annual/web-program/Manuscript/Paper262821/BJ-et-al-AMS-2015.pdf>
- Dickinson, R., Errico, R., Giorgi, F., Bates, G., 1989: A regional climate model for the western United States. *Clim. Chang.*, 15, 383-422.
- Dickinson, R.E., Henderson-Sellers, A., Kennedy, P.J., 1993: Biosphere-atmosphere Transfer Scheme (BATS) Version 1e as Coupled to the NCAR Community Climate Model. *NCAR Technical Note* NCAR/TN-387+STR, DOI: 10.5065/D67W6959
- Elguindi, N., Bi, X., Giorgi, F., Nagarajan, B., Pal, J., Solmon, F., Rauscher, S., Zakey, A., Giuliani, G., 2011: Regional climatic model RegCM user manual version 4.3. 32p. ITCP, Trieste, Italy.
- Giorgi, F., 1989: Two-dimensional simulations of possible mesoscale effects of nuclear war fires. 1. Model description. *J. Geophys. Res.*, 94, 1127-1144.
- Giorgi, F., Marinucci, M.R., Bates, G.T., 1993a: Development of a second generation regional climate model (RegCM2). Part I: Boundary layer and radiative transfer processes. *Mon. Wea. Rev.* 121, 2794-2813.
- Giorgi, F., Marinucci, M.R., Bates, G.T., DeCanio, G., 1993b: Development of a second generation regional climate model (RegCM2). Part II: Convective processes and assimilation of lateral boundary conditions. *Mon. Wea. Rev.* 121, 2814-2832.
- Giorgi, F., Mearns, L.O., 1999: Introduction to special section: regional climate modeling revisited *J. Geophys. Res.* 104, 6335-6352.
- Giorgi, F., Francisco, R., Pal, J., 2003: Effects of a subgrid-scale topography and land use scheme on the simulation of surface climate and hydrology. Part I: Effects of temperature and water vapor disaggregation. *J. Hydrometeor.*, 4(2): 317-333.
- Nakicenovic, N., Swart, R., Eds., 2000: *Emissions Scenarios*. A Special Reports of IPCC Working Group III, Cambridge University Press, Cambridge, UK. 570p.
- Pal, J.S., Small, E., Elthair, E., 2000: Simulation of regionalscale water and energy budgets: representation of subgrid cloud and precipitation processes within RegCM. *J. Geophys. Res.*, 105(29), 567-594.
- Pieczka, I., Pongrácz, R., André, K., Kelemen, F.D., Bartholy, J., 2016: Sensitivity analysis of different parameterization schemes using RegCM4.3 for the Carpathian Region. *Theoretical and Applied Climatology*, DOI 10.1007/s00704-016-1941-4
- Pongrácz, R., Bartholy, J., Kovács, G., Torma, Cs., 2010: Analysis of simulated mean and extreme climate trends for the Eastern/Central European region based on RegCM outputs using A1B scenario. In: *Proceedings, 90th AMS Annual Meeting*. Atlanta, GA. Paper 3.5, 7p. Available

- online at <http://ams.confex.com/ams/pdfpapers/158358.pdf>
- Pongrácz, R., Bartholy, J., Pieczka, I., Szabóné André, K., 2016: Estimation of regional climate changes in European and Mediterranean subregions using different RCP scenarios. In: *Proceedings, 96th AMS Annual Meeting*. New Orleans, LA. Paper 631, 5p. Available online at https://ams.confex.com/ams/96Annual/webprogram/Manuscript/Paper285411/Extended-paper-PR-BJ-PI-SZAK_2016_AMS.pdf
- Ruti, P.M., Somot, S., and the MedCORDEX modelling Team, 2016: Med-CORDEX initiative for Mediterranean climate studies. *Bull. Am. Meteor. Soc.*, 97, 1187-1208. DOI: 10.1175/BAMS-D-14-00176.1
- Somot, S., Ruti, P., and the MedCORDEX modelling Team, 2012: The Med-CORDEX initiative: towards fully coupled Regional Climate System Models to study the Mediterranean climate variability, change and impact. *Geophysical Research Abstracts*, 14, EGU2012-6080
- Torma, Cs., Coppola, E., Giorgi, F., Bartholy, J., Pongrácz, R., 2011: Validation of a high resolution version of the regional climate model RegCM3 over the Carpathian Basin. *J. Hydro-meteor.*, 12, 84-100.
- van Vuuren, D.P., Edmonds, J.A., Kainuma, M., Riahi, K., Thomson, A.M., Hibbard, K., Hurtt, G.C., Kram, T., Krey, V., Lamarque, J.-F., Masui, T., Meinshausen, M., Nakicenovic, N., Smith, S.J., Rose, S., 2011: The representative concentration pathways: an overview. *Climatic Change*, 109, 5-31. DOI: 10.1007/s10584-011-0148-z.